

1 **Diverse myeloid cells are recruited to the developing and inflamed mammary**
2 **gland**

3 Gillian J Wilson^{1,2}, Ayumi Fukuoka¹, Francesca Vidler¹ and Gerard J Graham¹.

4 ¹Chemokine Research Group, Institute of Infection, Immunity and Inflammation,
5 University of Glasgow, 120 University Place, Glasgow G12 8TA, UK.

6 ²To whom correspondence should be addressed:

7 Email: gillian.wilson@glasgow.ac.uk

8 Tel : +44 141 330 4741

9

10 **Running Title:** Recruitment of Mammary Myeloid Cells

11

12 **Keywords:** Mammary, Myeloid, Chemokine, development, inflammation.

13

14 **Abstract:**

15 The immune system plays fundamental roles in the mammary gland, shaping
16 developmental processes and controlling inflammation during infection and cancer.

17 Here we reveal unanticipated heterogeneity in the myeloid cell compartment during
18 development of virgin, pregnant and involuting mouse mammary glands, and in milk.

19 We investigate the functional consequences of individual and compound chemokine
20 receptor deficiency on cell recruitment. Diverse myeloid cell recruitment was also

21 shown in models of sterile inflammation and bacterial infection. Strikingly, we have
22 shown that inflammation and infection can alter the abundance of terminal end buds,

23 a key developmental structure, within the pubertal mammary gland. This previously

24 unknown effect of inflammatory burden during puberty could have important
25 implications for understanding the control of pubertal timing.

26

27

28

29

30

31

32

33

34

35

36

37

38

39

40

41

42

43

44 **Introduction:**

45 The mammary gland is a highly regenerative tissue within the body. It is unique, in that
46 most of its development occurs postnatally throughout the female reproductive
47 lifetime. The gland undergoes dramatic structural changes throughout puberty where
48 proliferative structures, terminal end buds (TEB), invade through the surrounding fatty
49 stroma, giving rise to a complex epithelial network in adulthood (MM Richert, KL
50 Schwertfeger, JW Ryder, 2000). During pregnancy, rapid proliferation of epithelial cells
51 generates lobuloalveoli (LAL), and milk producing ducts form during lactation. When
52 lactation stops upon weaning, a process of involution occurs where 90% of the gland
53 remodels to its pre-pregnancy form (MM Richert, KL Schwertfeger, JW Ryder, 2000).

54 The immune system has long been identified as a key component of the
55 mammary gland, residing within a stromal population containing fibroblasts,
56 extracellular matrix (ECM), and adipocytes (Wiseman and Werb, 2002). In particular,
57 macrophages play an essential role in regulating mammary gland branching
58 morphogenesis, as development is dramatically impaired in macrophage-deficient
59 mice (Pollard and Hennighausen, 1994; Gouon-Evans, Rothenberg and Pollard,
60 2000). In addition, the density of branching is reduced in CCL11 deficient mice, which
61 have decreased numbers of eosinophils (Gouon-Evans, Rothenberg and Pollard,
62 2000). Mast cell degranulation is also necessary for normal ductal development (Lilla
63 and Werb, 2010). The adaptive immune system plays an inhibitory role in the
64 regulation of pubertal development through CD11c+ antigen presenting cells and
65 CD4+ T cells (Plaks *et al.*, 2015). Neutrophils and dendritic cells are also key cell types
66 present in the gland during involution (Atabai, Sheppard and Werb, 2007; Betts *et al.*,
67 2018).

68 During inflammation, the immune cell landscape of the mammary gland is
69 altered. In breast cancer, immune cells infiltrate the gland, including tumour associated
70 macrophages (TAMs), Myeloid derived suppressor cells (MDSC), tumour associated
71 neutrophils (TANs), T-cells, and NK cells (Nagarajan and McArdle, 2018). Mastitis is
72 a common disease of the breast, caused by a build-up of milk in the ducts and
73 exacerbated by bacterial infection. Increased numbers of leukocytes including
74 neutrophils, monocytes and macrophages, are detected in the gland and in milk
75 (Hassiotou *et al.*, 2013; Cacho and Lawrence, 2017). This impacts milk quality, leading
76 to reduced infant weight gain and dysregulated immune development (Tuailon *et al.*,
77 2017) and often leads to early cessation of breastfeeding.

78 The molecular mechanisms which regulate the movement of immune cells as
79 they migrate within the gland to mediate their effects, are not fully understood. Insights
80 into these processes will enhance our understanding of how immune cells contribute
81 to mammary gland development and protect against inflammation. Chemokines,
82 characterised by a conserved cysteine motif, are a family of proteins important in cell
83 recruitment, and as *in vivo* regulators of intra-tissue cell movement. The chemokine
84 family is comprised of CC, CXC, XC and CX3C sub-families according to cysteine
85 distribution, and chemokines act through G-protein coupled receptors to facilitate
86 leukocyte migration (Nibbs and Graham, 2013). Inflammatory chemokine receptors
87 (iCCRs: CCRs1, 2, 3 and 5) are often expressed by immune cells and are required
88 for cell recruitment within the body (Douglas P. Dyer *et al.*, 2019). Previously we have
89 shown important roles for chemokine receptors in shaping the macrophage dynamics
90 within the mammary gland to control pubertal development (Wilson *et al.*, 2017, 2020).

91 Here we reveal unanticipated heterogeneity in myeloid cells within the
92 mammary gland at key developmental stages in virgin, pregnant and involuting mice.

93 We also reveal the myeloid cell composition of murine milk. In addition, we show that
94 diverse myeloid cells are recruited to the mammary gland during local inflammation
95 and remote infection. Importantly, we have shown that inflammation and infection alter
96 the number of terminal end buds, a key developmental structure, within the pubertal
97 mammary gland. The direct effect of inflammatory burden on pubertal development
98 has not been reported previously and could have important implications for
99 understanding the control of pubertal timing.

100

101

102

103

104

105

106

107

108

109

110

111

112

113

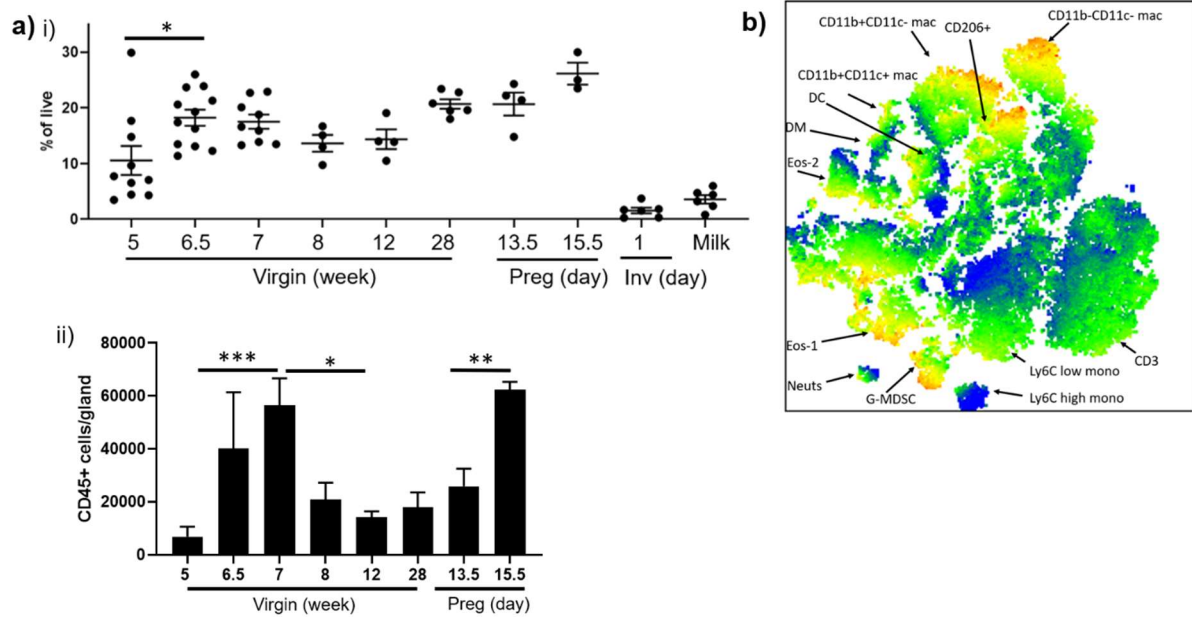
114 **Results:**

115 **Leukocyte levels in the mammary gland throughout development**

116 Flow cytometry was carried out to determine the levels of immune cells in the
117 mammary gland at key time points throughout virgin development, pregnancy and
118 involution, and in maternal milk. Leukocytes were defined as CD45+ and gated as
119 outlined in Supplementary Figure 1. The percentage of CD45+ cells within the live
120 population significantly increased between early (5 weeks) and late (6.5 weeks)
121 puberty (Figure 1ai). CD45+ cells represent a much lower percentage of live cells
122 within the gland on the first day of involution and in milk. The absolute number of
123 CD45+ cells per gland (Figure 1aii) was found to peak during late puberty at 7 weeks
124 in the virgin mammary gland and at day 15.5 during pregnancy. A detailed flow
125 cytometric analysis was carried out to identify myeloid cell types using a defined panel
126 of cell surface markers (Table 1, Supplementary Figure 1, 2). t-SNE analysis carried
127 out of CD45+ cells revealed distinct clusters corresponding to the cell types identified
128 (Figure 1 b).

129

130



131

132 **Figure 1: Leukocyte levels in the mammary gland throughout development. a)**

133 Flow cytometry of CD45+ cells in the mammary gland expressed as **i)** a percentage

134 of live cells during virgin development (5 weeks, n=10, 6.5 weeks, n=12, 7 weeks, n=9,

135 8 and 12 weeks, n=4, 28 weeks n=6) pregnancy (day 13.5, n=4, day 15.5, n=3)

136 involution (n=6) and in milk (n=6). **ii)** Total CD45+ cells per gland, during virgin

137 development (5 weeks, n=10, 6.5 weeks, n=3, 7 weeks, n=6, 8 and 12 weeks, n=4, 28

138 weeks n=6), and pregnancy (day 13.5, n=4, day 15.5, n=3). **b)** Representative tSNE

139 analysis of CD45+ cells within a sample from day 13.5 of pregnancy. Significantly

140 different results are indicated. Error bars represent S.E.M.

141

142

143

144

145

146 **Table 1: Myeloid cells within the mammary gland.**

| Cell Type | Surface Marker | | | | | | | |
|----------------------------|----------------|-------|-------|---------|------|------|-------|-------|
| | CD11b | CD11c | F4/80 | SiglecF | Ly6C | Ly6G | MHCII | CD206 |
| CD11b+F4/80+ Macrophage | + | | + | | | | | |
| CD206+ macrophage | | | + | - | | | | + |
| CD11b+CD11c+ macrophage | + | + | + | | | | + | |
| Ductal macrophage | - | + | + | | | | + | |
| CD11b-CD11c- macrophage | - | - | + | | | | + | |
| CD11b+CD11c- macrophage | + | - | + | | | | + | |
| Ly6C low monocyte | + | | | | low | - | | |
| Ly6C high monocyte | + | | | | high | | | |
| Eosinophil-1 | + | | + | + | | | | |
| Eosinophil-2 | + | | - | + | | | | |
| Neutrophil | + | | - | | | + | | |
| Dendritic cell | | + | - | | | | + | |
| G-MDSC | + | | + | | | + | | |

147

148

149

150

151

152

153

154 **Diverse macrophage subsets in the mammary gland throughout development.**

155 Macrophages play key roles in promoting mammary gland development and protecting
156 against disease. Classically mammary gland macrophages have been defined by
157 CD11b and F4/80 positivity. However recent studies have revealed further complexity
158 in the macrophage populations within the mammary gland. We identified a key
159 population of SiglecF-F4/80+CD206+ macrophages recruited by CCR1 which promote
160 branching morphogenesis during puberty (Wilson *et al.*, 2020). In addition, Dawson *et*
161 *al* identified a novel ductal macrophage important in tissue remodelling, defined as
162 CD11b-CD11c+MHCII+F4/80+(Dawson *et al.*, 2020). Here we reveal that in addition
163 to these subsets, there are three further populations, CD11b+CD11c+,
164 CD11b+CD11c- and CD11b-CD11c- macrophages (Table 1). The gating strategy
165 employed is shown in Supplementary Figure 1. We investigated the presence of each
166 of these subtypes in the gland throughout development and in milk.

167 CD11b+F4/80+ or 'classic' macrophages increase during puberty between 5 and 6.5
168 weeks (Figure 2 a). They represent a substantial proportion (approx. 20-30%) of the
169 CD45+ cells within the mammary gland through adulthood (8 weeks to 6 months) and
170 pregnancy. During early involution of the mammary gland and in breast milk they
171 represent only around 5% of CD45+ cells. This population can be further subdivided
172 into CD11c-MHCII+ (CD11b+CD11c-), and CD11c+MHCII+ (CD11b+CD11c+)
173 macrophages. CD11b+CD11c- macrophages are present at each stage of virgin
174 development and pregnancy, at a reduced level in early involution, but not in milk
175 (Figure 2 b). CD11b+CD11c+ macrophages are a small population which significantly
176 increase during puberty, between 5 and 6.5 weeks, and again during aging, between
177 12 and 28 weeks (Figure 2 c). They are detected at low levels during pregnancy,
178 involution and in milk (Figure 2 c).

179 We also identified a population of CD11b-CD11c- macrophages throughout
180 development which are found at the highest levels in early adulthood and pregnancy,
181 but not in milk (Figure 2 d). Ductal macrophages (CD11b-CD11c+) represent a low
182 percentage of CD45+ cells throughout virgin development and pregnancy. However,
183 in early involution they comprise around 20% of CD45+ cells (Figure 2 e). CD206+
184 macrophages represent a small proportion of CD45+ cells but have an important role
185 promoting branching morphogenesis in puberty (Wilson *et al.*, 2020). Here we show a
186 significant increase in this population between early (5 weeks) and late puberty (6.5
187 weeks) (Figure 2 f). They are also detected in the gland throughout adulthood,
188 pregnancy and involution, and in milk (Figure 2 f).

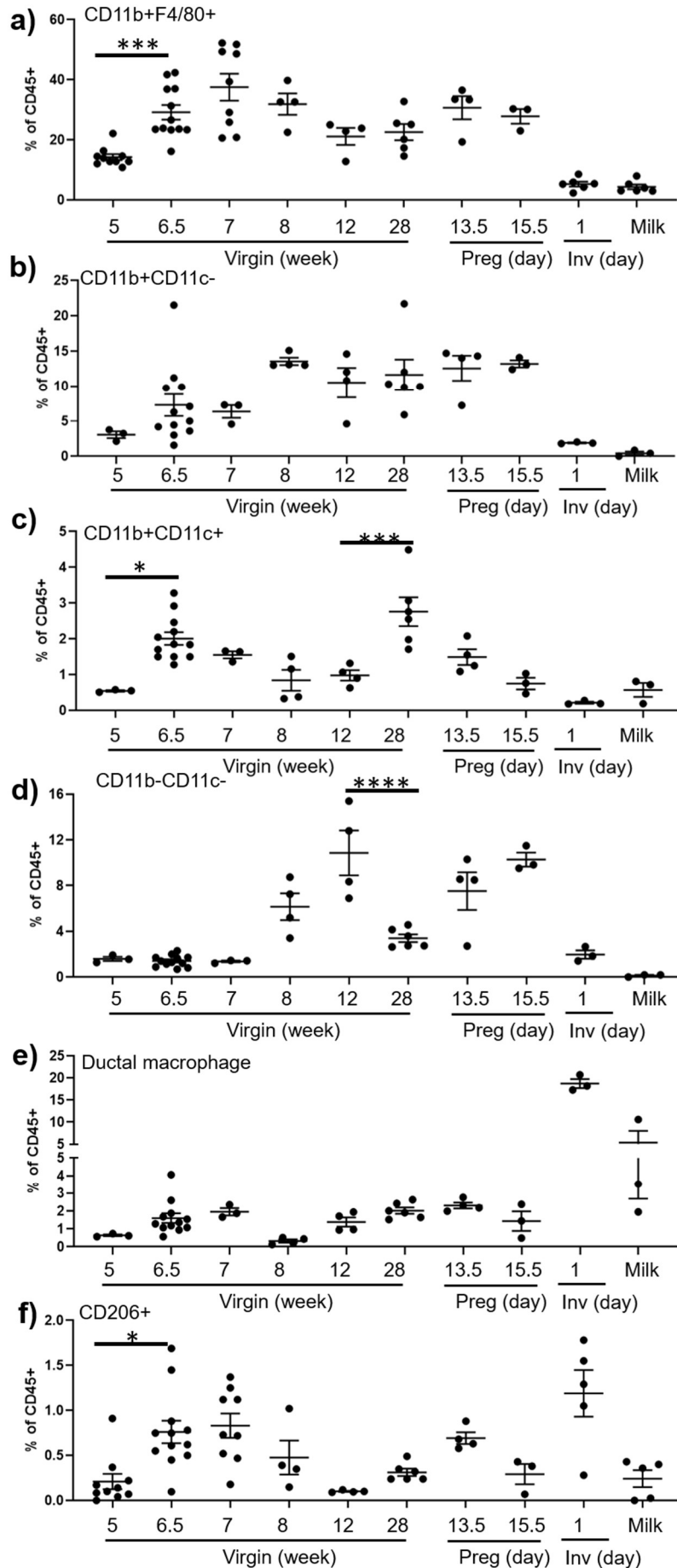
189

190

191

192

193



195 **Figure 2: Diverse macrophage subsets in the mammary gland throughout**
196 **development.** Flow cytometry was used to determine the percentage of **a)**
197 CD11b+F4/80+ macrophages, **b)** CD11b+CD11c-MHCII+F4/80+ macrophages, **c)**
198 CD11b+CD11c+MHCII+F4/80+ macrophages, **d)** CD11b-CD11c-MHCII+F4/80+
199 macrophages and **e)** CD11b-CD11c-MHCII+F4/80+ ductal macrophages, **f)** SiglecF-
200 F4/80+CD206+ macrophages within the CD45+ compartment of the mammary gland,
201 during virgin development, pregnancy, involution and in milk. **a, f)** virgin (5 weeks,
202 n=10, 6.5 weeks, n=12, 7 weeks, n=9, 8 and 12 weeks, n=4, 28 weeks n=6)
203 pregnancy (day 13.5, n=4, day 15.5, n=3) involution (n=6) and milk (n=6). **b-e)** virgin
204 (5 weeks, n=3, 6.5 weeks, n=12, 7 weeks, n=3, 8 and 12 weeks, n=4, 28 weeks n=6)
205 pregnancy (day 13.5, n=4, day 15.5, n=3) involution (n=3) and milk (n=3). Significantly
206 different results are indicated. Error bars represent S.E.M.

207

208

209

210

211

212

213

214

215

216

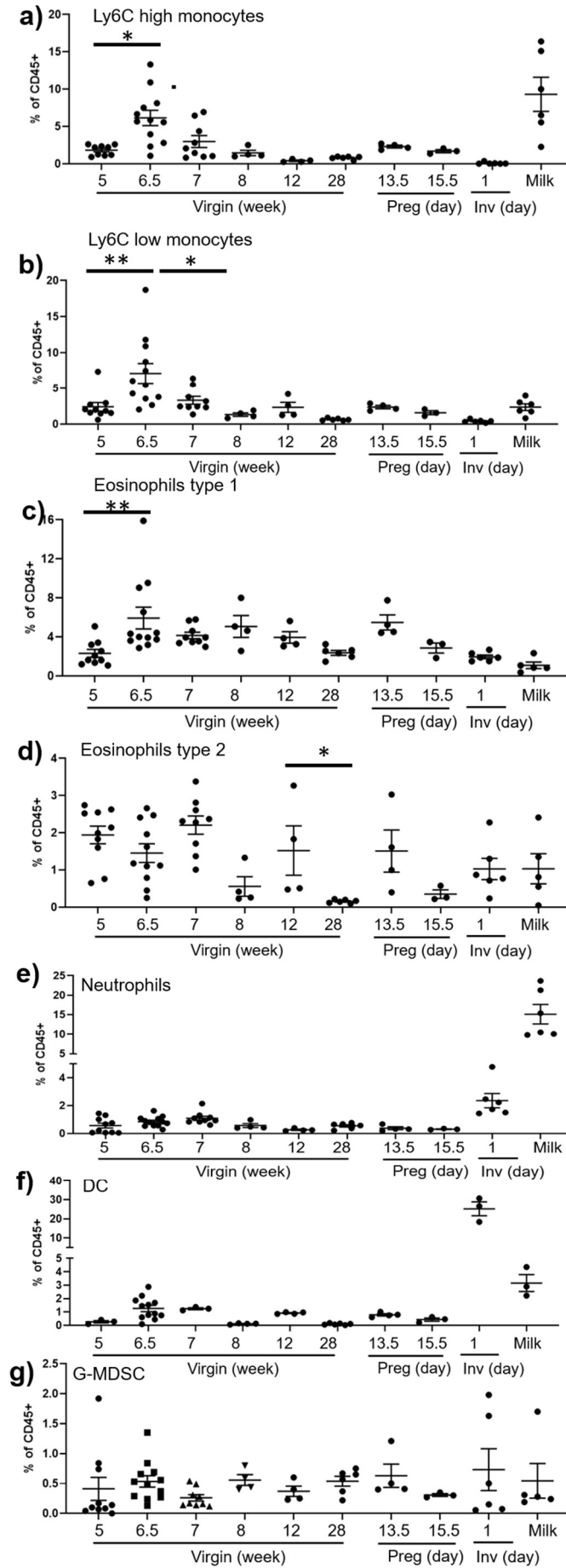
217 **Monocytes, granulocytes and dendritic cells in the mammary gland.**

218 We next examined the presence of further myeloid cell types in the mammary gland
219 using the gating strategy outlined in Supplementary Figure 2 and Table 1. There are
220 2 populations of monocytes in the mammary gland, Ly6C high and Ly6C low, which
221 increase in late puberty (Figure 3 a, b). Both monocyte subtypes are also found in
222 adult virgin and pregnant glands, at low levels during early involution and at higher
223 levels in milk (Figure 3 a, b). There are also 2 distinct populations of eosinophils
224 characterised by F4/80 expression. Type 1 eosinophils (F4/80+) represent a higher
225 percentage of CD45+ cells than type 2 (F4/80-) (Figure 3c, d). The percentage of type
226 1 but not type 2 eosinophils increases during late puberty. Both are detected in adult,
227 pregnant and involuting glands, and in milk (Figure 3c, d). Neutrophils are present at
228 low levels throughout virgin and pregnant gland development, but increase during
229 involution and represent a substantial proportion, around 15%, of leukocytes in milk
230 (Figure 3 e). Similarly, we have identified small numbers of dendritic cells (DCs)
231 throughout virgin and pregnant development, which dramatically rise during involution
232 (Figure 3 f). DCs are also detected in milk (Figure 3 f). A small population of
233 granulocytic myeloid derived suppressor cells (G-MDSC) was also detected at each
234 of the key developmental stages in the mammary gland, and in milk (Figure 3 g).

235 CSF1R is a marker for cells of the mononuclear phagocyte lineage including
236 macrophages, monocytes, and granulocytes (Sasamono et al, 2003). We carried out
237 flow cytometry of *MacGreen* (CSF1R GFP reporter) transgenic mice to confirm that
238 each of the cell types we have identified in the mammary gland are of myeloid origin
239 (Supplemental Figure 3 a). Surprisingly, we also found a small percentage of CD45
240 negative cells that are CSF1R positive (Supplemental Figure 3 b). Confocal imaging

241 and flow cytometric analysis reveal CSF1R expression by epithelial cells
242 (Supplemental Figure 3 b).

243



245 **Figure 3: Monocytes, granulocytes and dendritic cells in the mammary gland**
246 **throughout development.** Flow cytometry was used to determine the percentage of
247 **a) CD11b+Ly6C high monocytes b) CD11b+Ly6C low Ly6G- monocytes, c) Type 1**
248 **CD11b+SiglecF+ F4/80+ eosinophils d) Type 2 CD11b+SiglecF+ F4/80- eosinophils**
249 **e) F4/80-CD11b+Ly6G+ neutrophils, f) F4/80-CD11c+MHCII+ dendritic cells, and g)**
250 **F4/80+CD11b+Ly6G+ granulocytic myeloid derived suppressor cells (G-MDSC)**
251 **within the CD45+ compartment of the mammary gland, during virgin development,**
252 **pregnancy, involution and in milk. . a-e, g) virgin (5 weeks, n=10, 6.5 weeks, n=12, 7**
253 **weeks, n=9, 8 and 12 weeks, n=4, 28 weeks n=6) pregnancy (day 13.5, n=4, day**
254 **15.5, n=3) involution (n=6) and milk (n=6). f) virgin (5 weeks, n=3, 6.5 weeks, n=12,**
255 **7 weeks, n=3, 8 and 12 weeks, n=4, 28 weeks n=6) pregnancy (day 13.5, n=4, day**
256 **15.5, n=3) involution (n=3) and milk (n=3). Significantly different results are indicated.**
257 **Error bars represent S.E.M.**

258

259

260

261

262

263

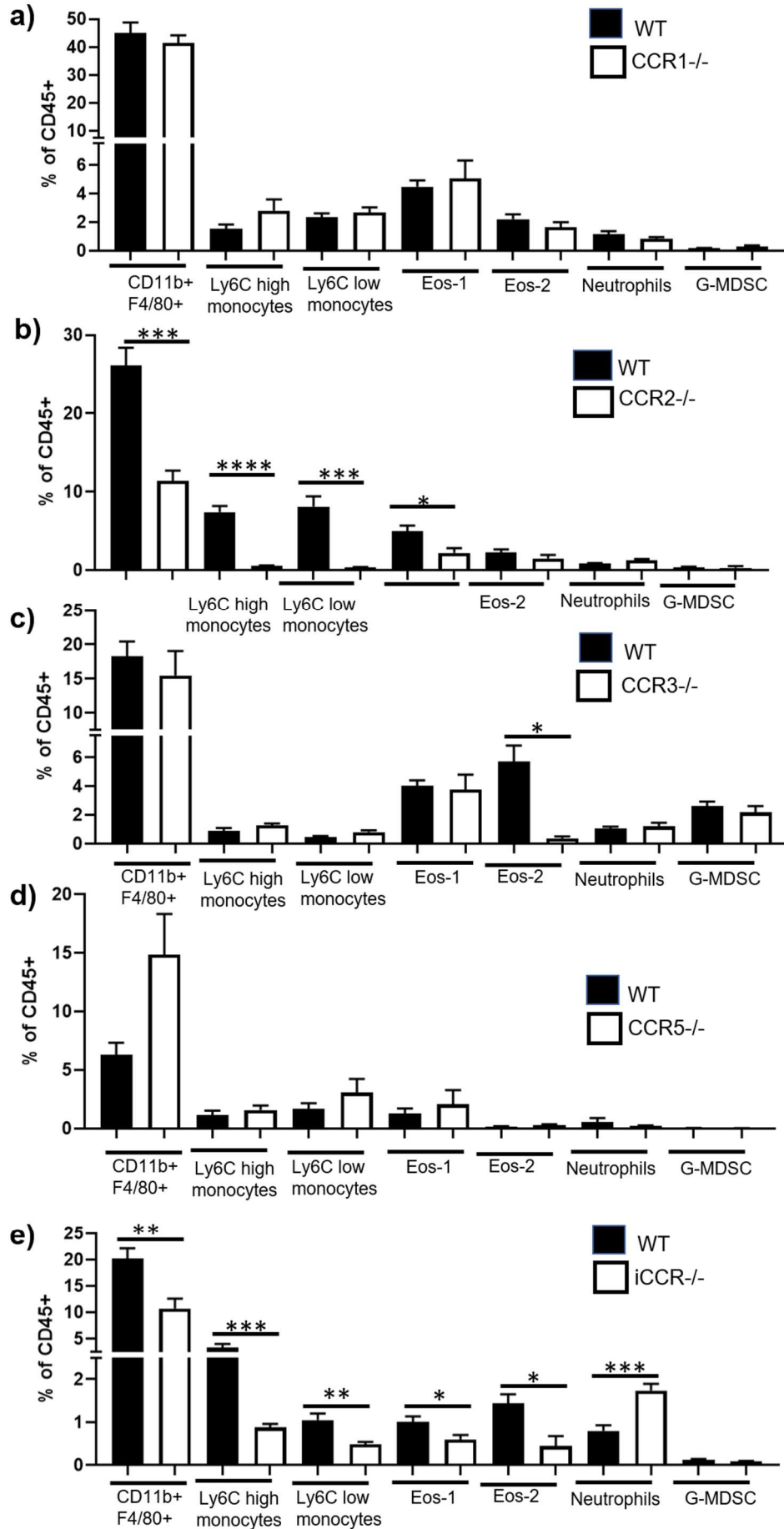
264

265

266

267 **iCCRs are required for cell recruitment to the mammary gland**

268 To investigate which iCCRs are required for the recruitment of myeloid cells to the
269 mammary gland, we analysed key cellular populations in WT, individual receptor
270 deficient mice, and mice with a compound receptor deletion of all four iCCRs, CCRs1,
271 2, 3 and 5. The receptor deficient mouse strains are on different genetic backgrounds
272 and therefore have been compared with their appropriate WT. Previously we revealed
273 that CD206+ macrophages are reduced in CCR1 deficient mice during late puberty (7
274 weeks)(Wilson *et al.*, 2020). There are no significant differences in any of the other
275 myeloid cell populations investigated in this study (Figure 4 a). In the absence of the
276 key monocyte receptor CCR2, both Ly6C high and Ly6C low monocytes are depleted
277 in 7 weeks old mice (Figure 4 b). We also observed a reduction in type 1 eosinophils
278 (Figure 4 b). Previously we observed that CD11b+F4/80+ cells were unaffected in
279 adult CCR2-/- mice (Wilson *et al.*, 2017), however in this study we observe a reduction
280 in CD11b+F4/80+ cells during puberty (Figure 4 b). In CCR3-/- mammary glands there
281 is a significant reduction in Type 2 eosinophils but not in any of the other populations
282 investigated. (Figure 4 c). In the absence of CCR5 we observed no differences in cell
283 recruitment (Figure 4 d). Importantly, in pubertal iCCR-/- mice which lack all 4
284 receptors, we also observed significant reductions in Ly6C high and Ly6C low
285 monocytes, type 1 and 2 eosinophils, and CD11b+F4/80+ macrophages. This
286 recapitulates the results of the individual receptor deficient mice and suggests there
287 are no additional combinatorial effects of compound receptor deficiency.



289 **Figure 4: iCCRs are required for cell recruitment to the mammary gland.** Flow
290 cytometry was used to determine the percentage of CD11b+F4/80+ macrophages,
291 Ly6C high monocytes, Ly6C low monocytes, type 1 (eos-1) and 2 (eos-2) eosinophils,
292 neutrophils and G-MDSC within the CD45+ compartment of the mammary gland
293 during virgin development of **a)** WT and CCR1^{-/-} (7 weeks, n=6 per group), **b)** WT (7
294 weeks, n=11) and CCR2^{-/-} (7 weeks, n=6), **c)** WT and CCR3^{-/-} (7 weeks, n=4 per
295 group), **d)** WT and CCR5^{-/-} (12 weeks, n=4 per group), **e)** WT and iCCR^{-/-} (7 weeks,
296 n=7 per group). Significantly different results are indicated. Error bars represent
297 S.E.M.

298

299

300

301

302

303

304

305

306

307

308

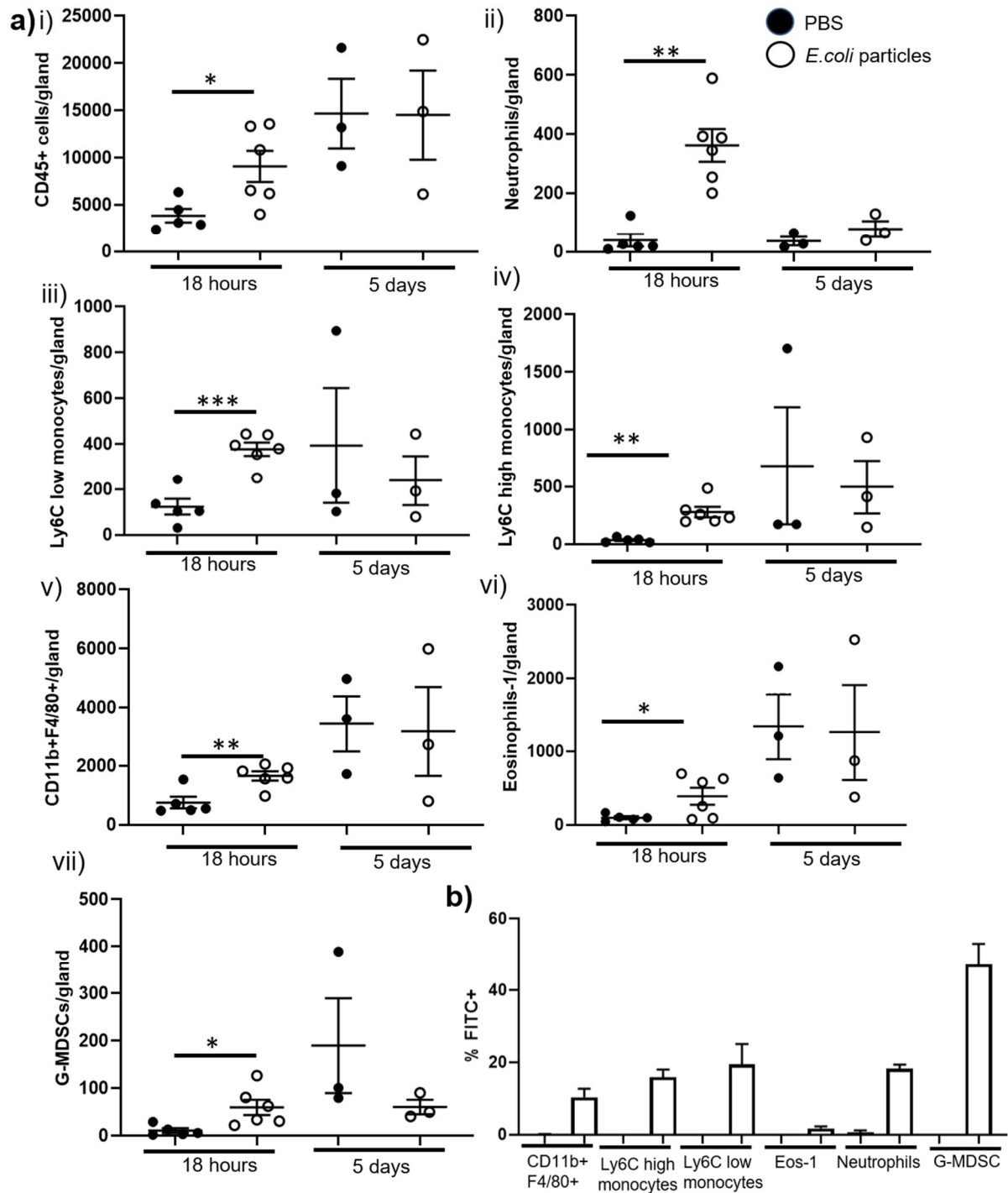
309

310

311 **Myeloid cells are recruited to the mammary gland during inflammation and**
312 **infection.**

313 To investigate the immune response in the mammary gland during local inflammation,
314 we injected mice during late puberty (6-7 weeks), subcutaneously at the site of the
315 mammary gland with either PBS or 500 µg of FITC labelled *Escherichia coli* particles
316 (ECP) for 18 h and 5 days. Cell recruitment to the mammary gland was measured by
317 flow cytometry. Overall, the number of CD45+ cells significantly increased 18 h after
318 challenge with ECP, with no difference observed in the resolution phase, after 5d
319 (Figure 5 a). Specifically, neutrophils, Ly6C high and Ly6C low monocytes,
320 CD11b+F4/80+ macrophages, type 1 eosinophils and G-MDSCs are all increased in
321 the mammary gland 18 h after challenge with ECP (Figure 5 a). In addition, we
322 observed binding of the FITC labelled ECP to each of these cell types (Figure 5 b).
323 After 5 days the number of cells was not significantly different and bound FITC labelled
324 ECP were not detected (Figure 5). We observed no change in recruitment of, or ECP
325 binding, to ductal CD11b+CD11c+, CD11b+CD11c-, CD11b-CD11c- or CD206+
326 macrophages, type 2 eosinophils or dendritic cells.

327 To investigate whether myeloid cells are altered in the mammary gland during a live
328 bacterial infection, 6-7 week old mice were infected intraperitoneally with 1×10^6 CFU
329 of a uropathogenic strain of *E.coli* (CFT073). 5 days after infection of the peritoneum,
330 the number of CD45+ cells within the mammary gland increased (Figure 6 a). As
331 observed during sterile inflammation, increased numbers of neutrophils, Ly6C low
332 monocytes and CD11b+F4/80+ macrophages were observed (Figure 6 b-d). We also
333 detected increased numbers of dendritic cells and CD206+ macrophages during
334 infection, which was not seen during sterile challenge (Figure 6 e-f).



335

336 **Figure 5: Myeloid cells are recruited to the mammary gland during sterile**

337 **inflammation.** Flow cytometry was used to determine **a)** the number of **i)** CD45+ cells,

338 **ii)** neutrophils, **iii)** CD11b+F4/80+ macrophages, **iv)** Ly6C low monocytes, **v)** Ly6C

339 high monocytes, **vi)** type 1 eosinophils (eos-1), and **vii)** G-MDSC within the mammary

340 gland after challenge with either PBS (denoted by black circles) or 500 µg of FITC

341 labelled *E.coli* particles (white circles), for 18h (PBS, n=5, *E.coli* particles, n=6) and 5
342 days (n=3 per group). **b)** The percentage of cells bound by FITC labelled *E.coli*
343 particles 18h after challenge (PBS, n=5, *E.coli* particles, n=6). Significantly different
344 results are indicated. Error bars represent S.E.M.

345

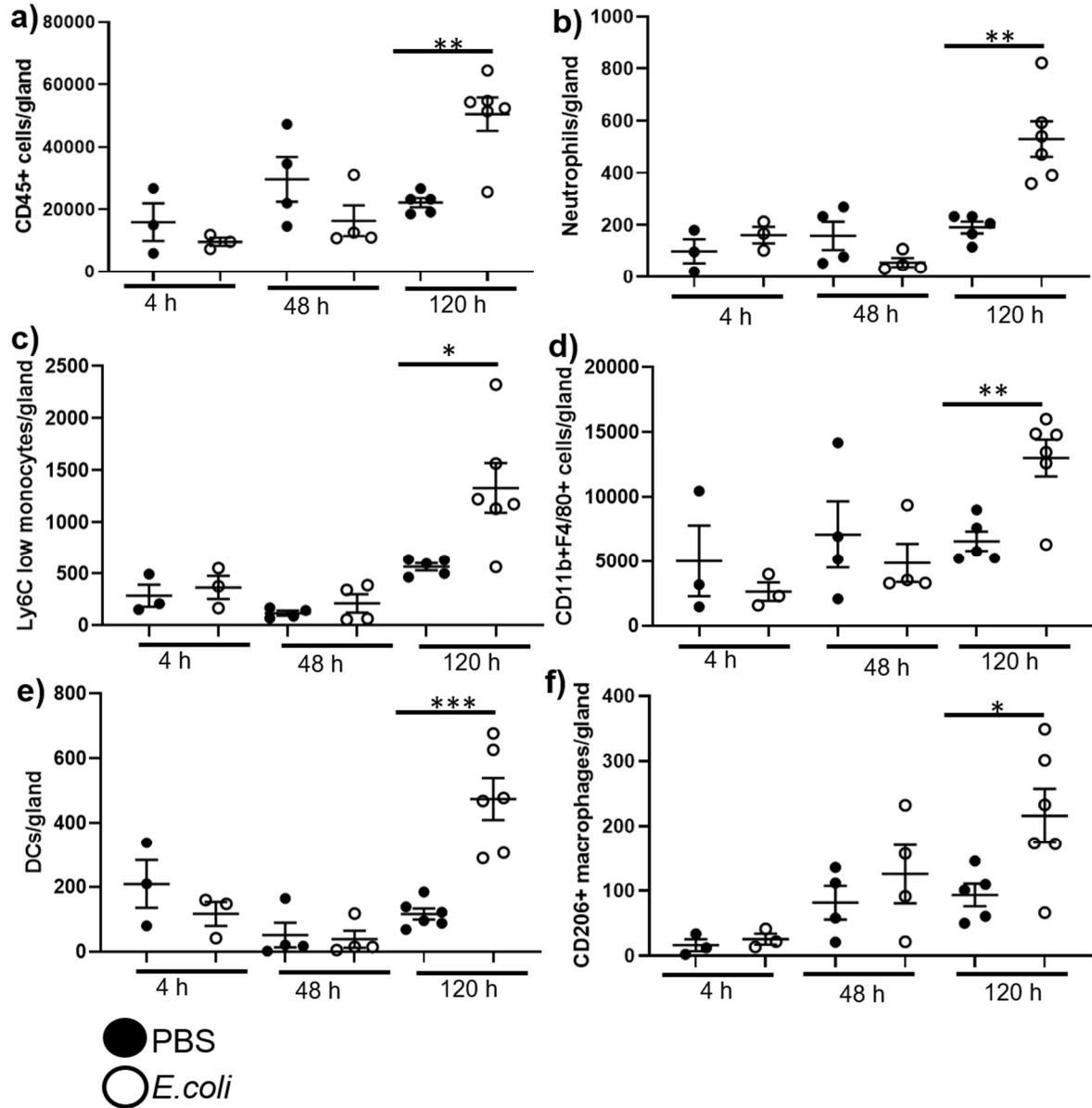
346

347

348

349

350



351

352 **Figure 6: Myeloid cells are recruited to the mammary gland during infection.**

353 Flow cytometry was used to determine the number of **a)** CD45+ cells, **b)** neutrophils,

354 **c)** Ly6C low monocytes, **d)** CD11b+F4/80+ macrophages, **e)** Dendritic cells, and **f)**

355 CD206+ macrophages within the mammary gland after intraperitoneal challenge with

356 either PBS (denoted by black circles) or 1×10^6 CFU *E. coli* strain CFT073 (white

357 circles), for 4 h (n=3 per group), 2 days (n=4 per group), and 5 days (PBS, n=5, *E. coli*,

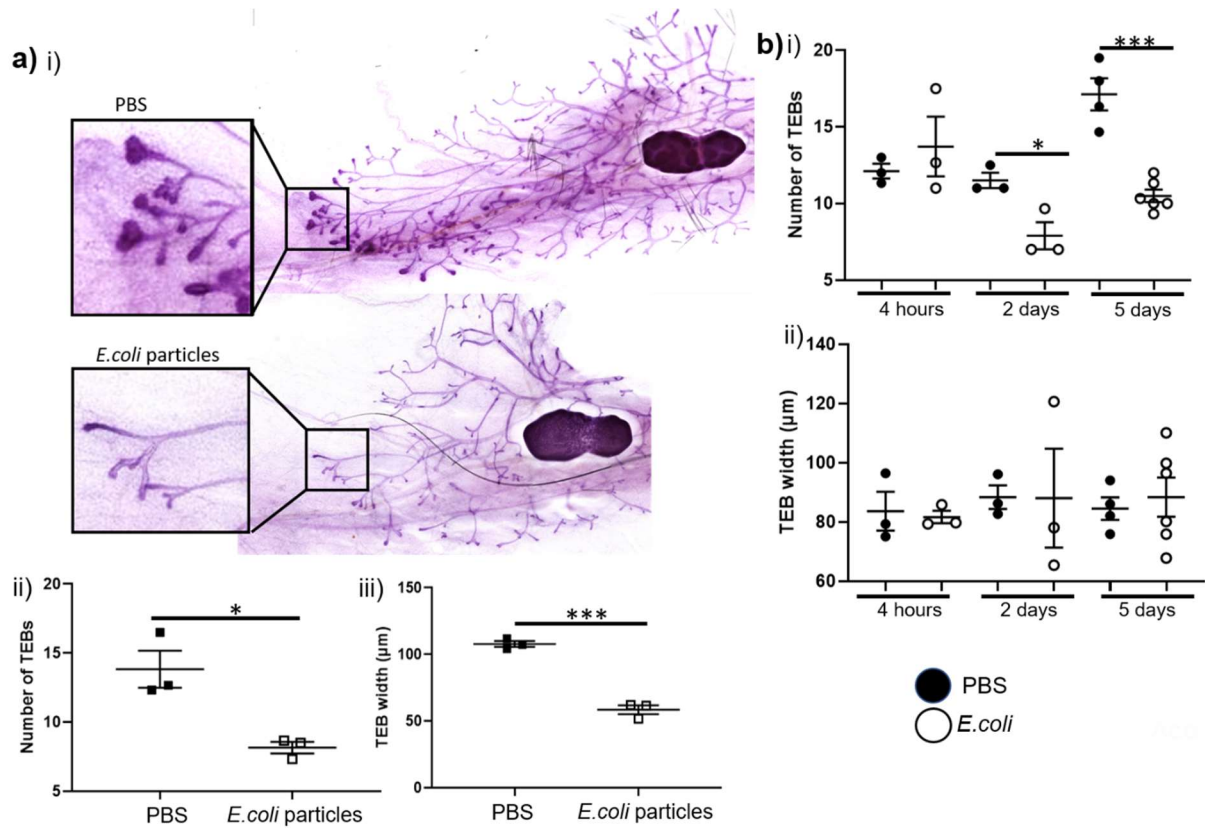
358 n=6). Significantly different results are indicated. Error bars represent S.E.M.

359

360 **Mammary gland structures are altered during infection and inflammation.**

361 We next investigated whether inflammation of the mammary gland altered
362 development of the gland during puberty. We analysed carmine alum stained whole-
363 mounts of mammary glands from pubertal WT mice challenged with either PBS, 200
364 μg ECP or 1×10^6 CFU *E.coli* CFT073 (Figure 7). TEBs are highly proliferative
365 structures within the pubertal mammary gland which give rise to the ductal epithelial
366 network within the gland. Strikingly we found that 3 d after intravenous challenge with
367 200 μg of ECP, the average number and width of terminal end buds was markedly
368 reduced (Figure 7 a). We also investigated the effect of live bacterial infection of the
369 peritoneum on TEB formation in the mammary gland and found that TEBs were
370 reduced 2 and 5 days after infection (Figure 7 bi). However, the morphology of the
371 TEB was not affected during peritoneal infection (Figure 7 bii).

372



373

374 **Figure 7: Mammary gland structures are altered during infection and**

375 **inflammation. a) i)** Representative carmine alum whole mount images (10 x) of

376 pubertal virgin mammary glands 3 days after intravenous challenge with PBS or 200

377 µg *E. coli* particles (ECP). **ii)** The number of terminal end buds (TEB) was determined

378 as the average number from at least 2 individual fields of view (FOV) (5x) per gland

379 and **iii)** the average width of all TEBs was determined from at least 2 F.O.V (5x) per

380 gland, 3 d after i.v challenge with PBS (denoted by black squares) or ECP (white

381 squares) (n=3 per group). **b) i)** The number of TEBs and **ii)** average width of all TEBs

382 after intraperitoneal challenge with either PBS (black circles) or 1×10^6 CFU *E. coli*

383 strain CFT073 (white circles), for 4 h (n=3 per group), 2 days (n=3 per group), and 5

384 days (PBS, n=4, *E. coli*, n=6). Significantly different results are indicated. Error bars

385 represent S.E.M.

386

387 **Discussion:**

388 Previously our understanding of immune system diversity within the mammary gland
389 in normal development has been limited. Here we provide a detailed analysis of the
390 myeloid cell landscape in the mouse mammary gland at key time points in
391 development and in murine milk. Macrophages are a particularly heterogeneous cell
392 type within the mammary gland. Recent studies have revealed novel subsets such as
393 the CD206+ macrophages which promote branching in late puberty (Jäppinen *et al.*,
394 2019; Wilson *et al.*, 2020), and ductal macrophages which cover the epithelium in
395 lactation and involution to facilitate remodelling (Dawson *et al.*, 2020). Here we have
396 used multi-parameter flow cytometry to reveal a further three macrophage subsets
397 within the mammary gland CD11b+CD11c+, CD11b+CD11c- and CD11b-CD11c-.
398 Further studies to investigate whether these macrophages have overlapping, or
399 distinct functions could reveal important insight into macrophage control of mammary
400 gland development and surveillance.

401 In addition, we have identified other important myeloid cell types in the
402 mammary gland. We believe this study represents the first full investigation of myeloid
403 cells throughout each of the key developmental stages. Although not exclusively, a
404 high proportion of mammary gland macrophages, at rest, and in inflammation, are
405 derived from monocytes in the bone marrow (Coussens and Pollard, 2011). Here we
406 reveal that both Ly6C high and Ly6C low monocytes are present in the developing
407 mammary gland at each stage, increasing significantly between early and late puberty.
408 In the absence of CCR2 both subtypes are depleted in the mammary gland.
409 Monocytes are also identified in established murine milk and likely contribute to
410 neonatal immune protection. We have also defined 2 types of eosinophil based on
411 F4/80 positivity. Type 1 (F4/80+) eosinophils only increase in late puberty and are

412 recruited through a CCR2 dependent mechanism. In contrast, type 2 (F4/80+)
413 eosinophils are recruited through CCR3 and are unchanged in puberty. To our
414 knowledge, our study is the first to describe the presence of small populations of
415 neutrophils, G-MDSC and DCs in the mammary gland of mice during virgin and
416 pregnant development. As has been reported previously, neutrophils are found at
417 higher numbers in early involution and are found at high levels in milk (Atabai,
418 Sheppard and Werb, 2007; Cacho and Lawrence, 2017).

419 We also carried out a detailed analysis of myeloid cell recruitment to the gland
420 in individual and compound iCCR deficient mice which lack all 4 receptors. We are
421 able to confirm that CCR2 is the dominant monocyte receptor in the mammary gland,
422 as has been observed throughout the body (Douglas P. Dyer *et al.*, 2019). Notably,
423 reduced recruitment of myeloid cells in iCCR^{-/-} mice corresponded with the cell types
424 reduced in individual receptor deficient mice. This suggests that there are no additional
425 combinatorial effects of multiple receptor deficiency.

426 Importantly, in this study we have revealed that local subcutaneous inflammation
427 and bacterial infection at a distant site with the body can have profound effects on the
428 immune cells present in the mammary gland. For the first time we have been able to
429 show that an inflammatory environment directly affects developmental structures
430 within the mammary gland. TEBs drive the formation of the ductal epithelial network
431 during puberty. Here we have shown that during inflammation and infection the
432 number of TEBs decreases. It has been shown that early breast development leads
433 to higher risks of breast cancer in later life (Bodicoat *et al.*, 2014), and women with
434 dense epithelial networks in the breast are more likely to develop breast cancer
435 (Nazari and Mukherjee, 2018). Thus, the potential to manipulate the immune system
436 to delay branching in puberty could have significant health benefits. There is evidence

437 to suggest that increased infections in early life lead to a delay in female puberty (Kwok
438 *et al.*, 2011). This previously unknown effect of inflammatory burden on mammary
439 structures during puberty could have important implications for understanding how
440 pubertal timing is controlled.

441

442

443

444

445

446

447

448

449

450

451

452

453

454

455

456

457 **Methods:**

458 **Animals**

459 Animal experiments were carried out under a UK Home Office Project Licence and
460 conformed to the animal care and welfare protocols approved by the University of
461 Glasgow. C57BL/6 mice, ACKR2^{-/-} (Jamieson *et al.*, 2005), CCR1^{-/-}, CCR3^{-/-}, CCR5^{-/-}
462 ^{-/-} and iCCR^{-/-} (Douglas P Dyer *et al.*, 2019), and *MacGreen* mice (Sasmono *et al.*,
463 2003) were bred at the specific pathogen-free facility of the Beatson Institute for
464 Cancer Research. All mice used for experiments in this study were female.

465 **Mammary gland digestion**

466 The inguinal lymph node was removed, and the fourth inguinal mammary gland was
467 chopped coarsely. Enzymatic digestion with 3 mg/ml collagenase type 1 (Sigma) and
468 1.5 mg/ml trypsin (Sigma) was carried out in a 37°C shaking incubator at 200 rpm for
469 1 h, in 2 ml Leibovitz L-15 medium (Sigma). Tissue was shaken for 10 s before 5 ml
470 of L-15 medium supplemented with 10% foetal calf serum (Invitrogen) was added.
471 Centrifugation was carried out at 400 g for 5 min. Red Blood Cell Lysing Buffer Hybri-
472 Max (Sigma) was applied for 1 min prior to washing in PBS containing 5 mM EDTA.
473 Cells were then resuspended in 2 ml 0.25% Trypsin-EDTA (Sigma) and incubated for
474 2 min at 37°C. Next 5 ml of L-15 containing 1 µg/ml DNase1 (Sigma) was added for 5
475 min at 37°C. L-15 containing 10% FCS was then added to stop the reaction and cells
476 were filtered through a 40 µm cell strainer. Finally, cells were washed in FACS buffer
477 (PBS containing 1% FCS and 5 mM EDTA). Milk was obtained by removing mammary
478 glands from lactating mice at day 7. Mammary glands were placed intact in FACS
479 buffer and milk was collected, washed and stained.

480

481 **Flow cytometry**

482 Antibodies were obtained from BioLegend and used at a dilution of 1:200: CD45 (30-
483 F11), CD11b (M1/70), F4/80 (BM8), SiglecF (S17007L), Ly6C (HK1.4), CD11c (N418),
484 MHCII (M5/114.15.2), EpCAM (G8.8), CD49f(GoH3), and CD206 (C068C2) for 30 min
485 at 4°C. Ly6G (1A8) was obtained from BD Bioscience. Dead cells were excluded using
486 Fixable Viability Dye eFluor 506 (Thermo Fisher). Flow cytometry was performed using
487 a Fortessa, (BDBiosciences) and analysed using FlowJo V10.

488

489 **Sterile Inflammation of the mammary gland**

490 Female mice between 6-7 weeks of age were injected subcutaneously with 500 µg, or
491 intravenously with 200 µg of FITC labelled *E.coli* (K-12 strain) Bioparticles in 200 µl
492 PBS (Thermo). After a defined number of days, mice were culled and mammary
493 glands were excised and processed for whole mount and cellular analysis.

494

495 **Peritoneal bacterial infection**

496 Female mice between 6-7 weeks of age were injected intraperitoneally with 1×10^6 CFU
497 of *E.coli* (CFT073 strain). Bacteria were grown overnight in Luria-Bertani medium,
498 before being sub-cultured and grown to log phase for injection ($OD_{600} = 0.5$, 5×10^8
499 CFU/ml). Mice were monitored for weight loss and clinical signs of infection. Mice were
500 culled and mammary glands were excised and processed for whole mount and cellular
501 analysis.

502

503 **Carmine Alum Whole Mount**

504 Carmine alum whole mounts were carried out as previously described (Wilson *et al.*,
505 2017, 2020). Briefly, fourth inguinal mammary glands were fixed in 10% neutral
506 buffered formalin (NBF) (Leica) overnight at 4°C. Glands were dehydrated for 1 h in
507 distilled water, then 1 h 70% ethanol and 1 h 100% ethanol before incubation in xylene
508 overnight (VWR international). Rehydrated was achieved by 1 h incubation in 100%
509 ethanol, 70% ethanol and distilled water, before staining with Carmine Alum solution
510 at room temperature overnight (0.2% (w/v) carmine and 10 mM aluminium potassium
511 sulphate (Sigma)). Tissue was dehydrated again and incubated overnight in xylene.
512 Glands were then mounted with DPX (Leica) and 10× magnification stitched bright-
513 field images were obtained using an EVOS FL auto2 microscope (Thermofisher). 5 x
514 brightfield images were obtained using the Zeiss Axioimager M2 with Zen 2012
515 software. TEBs were counted as the average from at least 2 F.O.V. from each whole
516 mount. All samples were blinded before measurements were taken.

517 **Statistical analysis**

518 Data were analysed using GraphPad Prism 8.1.2. Normality was assessed using
519 Shapiro Wilk and Kolmogorov–Smirnov tests. For normally distributed data, two-tailed,
520 unpaired t-tests were used. Where data was not normally distributed, Mann–Whitney
521 tests were used. Multiple comparison analysis was carried out using an ANOVA with
522 Tukey’s post-test. Significance was defined as $p < 0.05$ *. Error bars indicate standard
523 error of the mean (S.E.M.).

524 **Funding**

525 This study was supported by a Programme Grant from the Medical Research Council
526 (MR/M019764/1) and a Wellcome Trust Investigator Award ([099251/Z/12/Z](#)).

527

528 **Author Contributions**

529 GJW conceived the study, performed experiments, analysed data and wrote the
530 paper. AF and FV performed experiments. GJG conceived the study and wrote the
531 paper.

532 **Acknowledgments:**

533 We thank the University of Glasgow's animal facility staff for the care of our animals
534 and flow cytometry facility staff for technical assistance. We thank Prof. Andy Roe for
535 providing *E.coli* CFT073. The study was supported by a Programme Grant from the
536 Medical Research Council (MR/M019764/1). Work in GJG's laboratory is also funded
537 by a Wellcome Trust Investigator Award ([099251/Z/12/Z](#)). GJG is a recipient of a
538 Wolfson Royal Society Merit award.

539 **Competing Interests**

540 The authors declare no competing interests.

541

542

543

544

545

546

547

548

549

550 **References:**

551 Atabai, K., Sheppard, D. and Werb, Z. (2007) 'Roles of the Innate Immune System in
552 Mammary Gland Remodeling During Involution', *Journal of Mammary Gland Biology
553 and Neoplasia*, 12(1), pp. 37–45. doi: 10.1007/s10911-007-9036-6.

554 Betts, C. B., Pennock, N. D., Caruso, B. P., Ruffell, B., Borges, V. F. and Schedin, P.
555 (2018) 'Mucosal Immunity in the Female Murine Mammary Gland', *The Journal of
556 Immunology*, 201(2), pp. 734 LP – 746. doi: 10.4049/jimmunol.1800023.

557 Bodicoat, D. H., Schoemaker, M. J., Jones, M. E., McFadden, E., Griffin, J.,
558 Ashworth, A. and Swerdlow, A. J. (2014) 'Timing of pubertal stages and breast
559 cancer risk: the Breakthrough Generations Study', *Breast Cancer Research*, 16(1),
560 p. R18. doi: 10.1186/bcr3613.

561 Cacho, N. T. and Lawrence, R. M. (2017) 'Innate Immunity and Breast Milk',
562 *Frontiers in Immunology*, 8, p. 584. doi: 10.3389/fimmu.2017.00584.

563 Coussens, L. M. and Pollard, J. W. (2011) 'Leukocytes in mammary development
564 and cancer', *Cold Spring Harbor perspectives in biology*. Cold Spring Harbor
565 Laboratory Press, 3(3), p. a003285. doi: 10.1101/cshperspect.a003285.

566 Dawson, C. A., Pal, B., Vaillant, F., Gandolfo, L. C., Liu, Z., Bleriot, C., Ginhoux, F.,
567 Smyth, G. K., Lindeman, G. J., Mueller, S. N., Rios, A. C. and Visvader, J. E. (2020)
568 'Tissue-resident ductal macrophages survey the mammary epithelium and facilitate
569 tissue remodelling', *Nature Cell Biology*, 22(5), pp. 546–558. doi: 10.1038/s41556-
570 020-0505-0.

571 Dyer, Douglas P., Medina-Ruiz, L., Bartolini, R., Schuette, F., Hughes, C. E., Pallas,

- 572 K., Vidler, F., Macleod, M. K. L., Kelly, C. J., Lee, K. M., Hansell, C. A. H. and
573 Graham, G. J. (2019) 'Chemokine Receptor Redundancy and Specificity Are Context
574 Dependent', *Immunity*. Cell Press, 50(2), pp. 378-389.e5. doi:
575 10.1016/J.IMMUNI.2019.01.009.
- 576 Dyer, Douglas P, Medina-Ruiz, L., Bartolini, R., Schuette, F., Hughes, C. E., Pallas,
577 K., Vidler, F., Macleod, M. K. L., Kelly, C. J., Lee, K. M., Hansell, C. A. H. and
578 Graham, G. J. (2019) 'Chemokine Receptor Redundancy and Specificity Are Context
579 Dependent', *Immunity*, 50(2), pp. 378-389.e5. doi:
580 <https://doi.org/10.1016/j.immuni.2019.01.009>.
- 581 Gouon-Evans, V., Rothenberg, M. E. and Pollard, J. W. (2000) 'Postnatal mammary
582 gland development requires macrophages and eosinophils', *Development*, 127(11),
583 pp. 2269 LP – 2282. Available at:
584 <http://dev.biologists.org/content/127/11/2269.abstract>.
- 585 Hassiotou, F., Hepworth, A. R., Metzger, P., Tat Lai, C., Trengove, N., Hartmann, P.
586 E. and Filgueira, L. (2013) 'Maternal and infant infections stimulate a rapid leukocyte
587 response in breastmilk', *Clinical & translational immunology*. Nature Publishing
588 Group, 2(4), pp. e3–e3. doi: 10.1038/cti.2013.1.
- 589 Jamieson, T., Cook, D. N., Nibbs, R. J. B., Rot, A., Nixon, C., Mclean, P., Alcamí, A.,
590 Lira, S. A., Wiekowski, M. and Graham, G. J. (2005) 'The chemokine receptor D6
591 limits the inflammatory response in vivo', *Nature Immunology*, 6(4), pp. 403–411. doi:
592 10.1038/ni1182.
- 593 Jäppinen, N., Félix, I., Lokka, E., Tyystjärvi, S., Pynttari, A., Lahtela, T., Gerke, H.,
594 Elima, K., Rantakari, P. and Salmi, M. (2019) 'Fetal-derived macrophages dominate
595 in adult mammary glands', *Nature Communications*, 10(1), p. 281. doi:

596 10.1038/s41467-018-08065-1.

597 Kwok, M. K., Leung, G. M., Lam, T. H. and Schooling, C. M. (2011) 'Early Life
598 Infections and Onset of Puberty: Evidence From Hong Kong's Children of 1997 Birth
599 Cohort', *American Journal of Epidemiology*, 173(12), pp. 1440–1452. doi:
600 10.1093/aje/kwr028.

601 Lilla, J. N. and Werb, Z. (2010) 'Mast cells contribute to the stromal
602 microenvironment in mammary gland branching morphogenesis', *Developmental
603 Biology*, 337(1), pp. 124–133. doi: <https://doi.org/10.1016/j.ydbio.2009.10.021>.

604 MM Richert, KL Schwertfeger, JW Ryder, S. A. (2000) 'An atlas of mouse mammary
605 gland development.', *Journal of Mammary Gland Biology and Neoplasia*, 2, pp. 227–
606 241. Available at: <https://link.springer.com/article/10.1023/A:1026499523505>.

607 Nagarajan, D. and McArdle, S. E. B. (2018) 'Immune Landscape of Breast Cancers',
608 *Biomedicines*, 6.

609 Nazari, S. S. and Mukherjee, P. (2018) 'An overview of mammographic density and
610 its association with breast cancer', *Breast cancer (Tokyo, Japan)*. 2018/04/12.
611 Springer Japan, 25(3), pp. 259–267. doi: 10.1007/s12282-018-0857-5.

612 Nibbs, R. J. B. and Graham, G. J. (2013) 'Immune regulation by atypical chemokine
613 receptors', *Nature Reviews Immunology*. Nature Publishing Group, a division of
614 Macmillan Publishers Limited. All Rights Reserved., 13, p. 815. Available at:
615 <https://doi.org/10.1038/nri3544>.

616 Plaks, V., Boldajipour, B., Linnemann, J. R., Nguyen, N. H., Kersten, K., Wolf, Y.,
617 Casbon, A.-J., Kong, N., van den Bijgaart, R. J. E., Sheppard, D., Melton, A. C.,
618 Krummel, M. F. and Werb, Z. (2015) 'Adaptive Immune Regulation of Mammary

- 619 Postnatal Organogenesis', *Developmental Cell*. Elsevier, 34(5), pp. 493–504. doi:
620 10.1016/j.devcel.2015.07.015.
- 621 Pollard, J. W. and Hennighausen, L. (1994) 'Colony stimulating factor 1 is required
622 for mammary gland development during pregnancy', *Proceedings of the National
623 Academy of Sciences*, 91(20), pp. 9312 LP – 9316. doi: 10.1073/pnas.91.20.9312.
- 624 Sasmono, R. T., Oceandy, D., Pollard, J. W., Tong, W., Pavli, P., Wainwright, B. J.,
625 Ostrowski, M. C., Himes, S. R. and Hume, D. A. (2003) 'A macrophage colony-
626 stimulating factor receptor–green fluorescent protein transgene is expressed
627 throughout the mononuclear phagocyte system of the mouse', *Blood*, 101(3), pp.
628 1155 LP – 1163. doi: 10.1182/blood-2002-02-0569.
- 629 Tuailon, E., Viljoen, J., Dujols, P., Cambonie, G., Rubbo, P.-A., Nagot, N., Bland, R.
630 M., Badiou, S., Newell, M.-L. and Van de Perre, P. (2017) 'Subclinical mastitis
631 occurs frequently in association with dramatic changes in inflammatory/anti-
632 inflammatory breast milk components', *Pediatric Research*, 81(4), pp. 556–564. doi:
633 10.1038/pr.2016.220.
- 634 Wilson, G. J., Fukuoka, A., Love, S. R., Kim, J., Pinggen, M., Hayes, A. J. and
635 Graham, G. J. (2020) 'Chemokine receptors coordinately regulate macrophage
636 dynamics and mammary gland development', *Development*, 147(12), p. dev187815.
637 doi: 10.1242/dev.187815.
- 638 Wilson, G. J., Hewit, K. D., Pallas, K. J., Cairney, C. J., Lee, K. M., Hansell, C. A.,
639 Stein, T. and Graham, G. J. (2017) 'Atypical chemokine receptor ACKR2 controls
640 branching morphogenesis in the developing mammary gland', *Development
641 (Cambridge)*, 144(1). doi: 10.1242/dev.139733.
- 642 Wiseman, B. S. and Werb, Z. (2002) 'Stromal Effects on Mammary Gland

643 Development and Breast Cancer', *Science*, 296(5570), pp. 1046 LP – 1049. doi:

644 10.1126/science.1067431.

645